Cascading Dark Energy

Amjad Ashoorioon (Physics, IPM)

The 27st international symposium on Particles, Strings and Cosmology
(PASCOS 2022)
July 26th , 2022

Based on
a work in progress
with
Kazem Rezazadeh (IPM, Tehran)
&
Daniel Grin (Haverford College)

IPM
پژوهشگاه دانش‌های بنیادی

Introduction

- **Hubble Tension:**

  - Measurements of H_0 including CMB data from Planck 2018, BAO, DES, and BBN, fitted to the ΛCDM, predict $H_0 = 67.4 \pm 0.6$ km s^{-1} Mpc^{-1}.

    Aghanim et al. (2020)

    Abbott et al. (2018)

  - Measurements of H_0 tethered to distance ladder obtained using Hubble Space Telescope (HST) observations of 70 long-period Cepheids in the Large Magellanic Cloud, $H_0 = 74.03 \pm 1.42$ km s^{-1} Mpc^{-1}.

    Riess et al. (2019)

  - This is known as the Hubble tension which has put the concordance model in the midst of a crisis.

Introduction

- Origin of Hubble tension may be systematics, BUT
- It can also herald New Physics beyond the ΛCDM:
  - Late time Solutions: Modifications of ΛCDM close to today:
    - Phantom Dark Energy
    - Vacuum Phase Transition at Late times
    - Interacting Dark Energy
    - Model-independent parameterization of the late-time cosmology
    - Late-time modifications of modified theories of gravity.
- Constrained tightly by CMB and the late time observations such as BAO and conflicts with the age of the globular clusters.

Introduction

- Early time resolutions: introduce a scalar component whose energy redshifts like or faster than radiation before matter-radiation equality.
  - increases the expansion rate of the Universe at early times (reducing the sound horizon) while leaving the later evolution of the Universe unchanged.
  - Constrained by BAO and high ℓ C_ℓ's.
  - In one of the early realizations, the scalar field component has to redshift faster than radiation.

V. Poulin et al. PRL (2019)

T. Smith et al. PRD (2020)

Introduction

- σ_8 **(or S_8) Tension:**

- $S_8 \equiv \sigma_8 \sqrt{\frac{\Omega_m}{0.3}}$ where σ_8 is the amplitude of matter perturbations within 8 Mpc/h and Ω_m is the matter density today.

- Again there is a discrepancy between the CMB results and local measurements, such as the DES three year survey of the matter density perturbation

$$S_8^{\mathrm{DES}} = 0.797^{+0.015}_{-0.013} \; (68\,\%\,\mathrm{C.L.}) \qquad S_8^{\mathrm{Planck}} = 0.832 \pm 0.013 \; (68\,\%\,\mathrm{C.L.})$$

Assuming ΛCDM

- The EDE models tend to worsen the S_8 tension and fitting with the BAO data.

Introduction

- Model of dark energy which is *motivated* by the Swampland conjecture in String Theory.
- The whole dark energy phenomenon is from the cooperation of many fields.
- However one of the fields is not in sync with the other ones.
- It cascades sooner than the rest and oscillates around its minimum,
- This cascading process leads to the enhancement of H_0

Setup

- Let us consider $N+1$ scalar fields:

$$S = \int d^4x\sqrt{-g}\left[\sum_{i=1}^{N+1}\left(\frac{1}{2}\partial_\mu\phi_i\partial^\mu\phi_i - \frac{\lambda}{4}\phi_i^4\right)\right] .$$

- We took the potential of all the fields to be quartic monomials.
- Now the Swampland distance conjecture, articulates that $\phi_i \lesssim M_P$
- Now in this limit, the dS swampland conjecture is always satisfied

$$M_P\frac{V'}{V} \gtrsim c = \mathcal{O}(1)$$

Setup

- Now let us assume that all the N fields have approached the same initial condition, which is different from the secluded field.

$$\phi_1 = \phi_2 = \ldots = \phi_N = \phi_0 \,,$$
$$\phi_{N+1} = \chi_0 \,.$$

$\forall\ i \in \{1,\ldots,N+1\},\ \ \phi_i \lesssim M_P$

$$S = \int d^4x \sqrt{-g} \left(\frac{N}{2} \partial_\mu \phi_0 \partial^\mu \phi_0 + \frac{1}{2} \partial_\mu \chi_0 \partial^\mu \chi_0 - N \frac{\lambda}{4} \phi_0^4 - \frac{\lambda}{4} \chi^4 \right) .$$

- Let us introduce the variables $\phi \equiv \sqrt{N} \phi_0$ $\chi \equiv \chi_0$

$$S = \int \sqrt{-g}\, d^4x \left(\frac{1}{2} \partial_\mu \phi \partial^\mu \phi + \frac{1}{2} \partial_\mu \chi \partial^\mu \chi - \frac{\lambda_\phi}{4} \phi^4 - \frac{\lambda_\chi}{4} \chi^4 \right)$$

where $\lambda_\phi \equiv \dfrac{\lambda}{N}$ $\lambda_\chi \equiv \lambda$

- If $N \gg 1$, we expect that $\lambda_\chi \gg \lambda_\phi$ and $\chi \lesssim M_P \lesssim \phi$

Setup

- When $m_\chi^2 \equiv V_{\chi\chi} \gtrsim H^2$, the χ field starts rolling. This will lead to the sudden drop of the comoving sound horizon before decoupling, which enhances H_0.

- Similar setup could be arranged within the multi-giant matrix models.

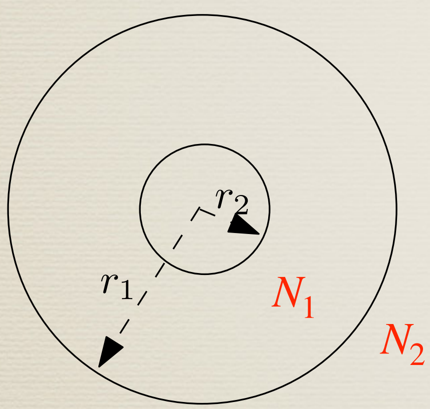

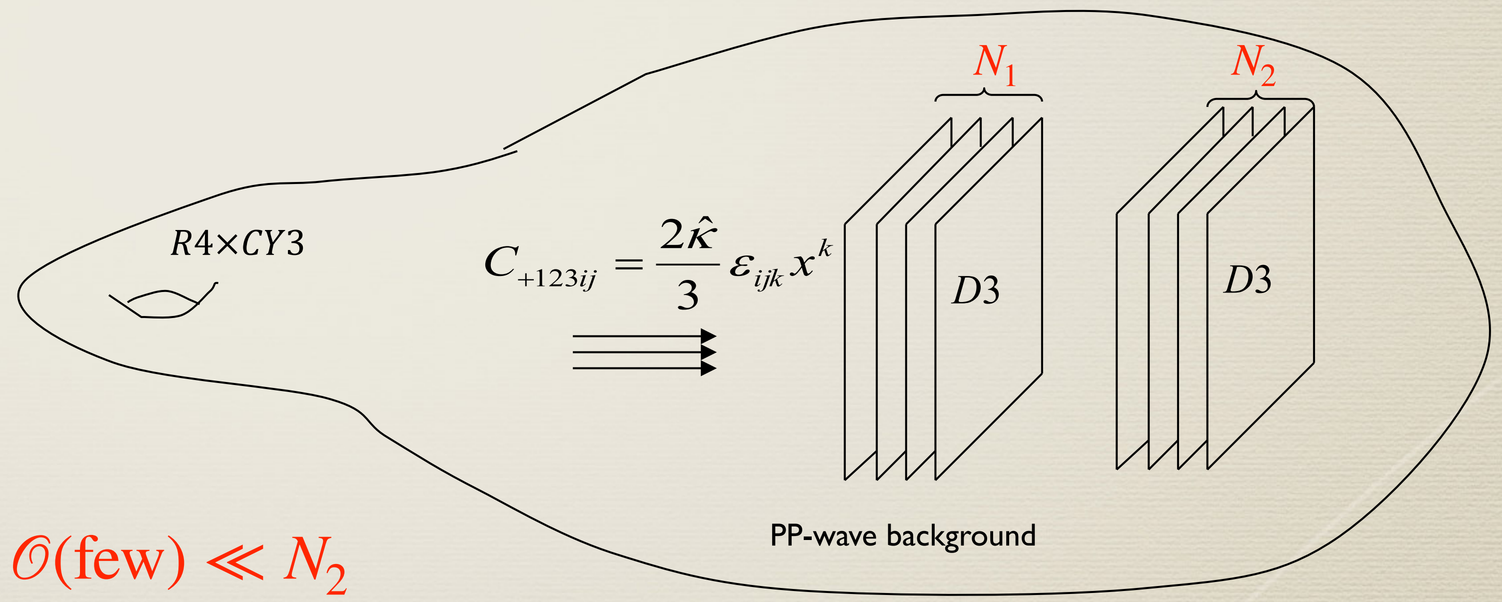

$$V(\phi_\alpha) = \sum_\alpha \frac{\lambda_\alpha}{4}\phi_\alpha^4 - \frac{2\kappa_\alpha}{3}\phi_\alpha^3 + \frac{m^2}{2}\phi_\alpha^2$$

$$\lambda_\alpha = \frac{8\lambda}{N_\alpha(N_\alpha^2-1)}\,, \qquad \kappa_\alpha = \frac{2\kappa}{\sqrt{N_\alpha(N_\alpha^2-1)}}.$$

$N_1 \sim \mathcal{O}(\text{few}) \ll N_2$

$\lambda \sim 1 \quad \lambda = 8\pi g_s \longrightarrow N_2 \sim 10^{40}$

Setup

- Alternatively one can assume that $g_s \sim \mathcal{O}(10^{-100})$ and obtain further suppression through the D3 branes multiplicity.

- One can also reduce the number of D3 branes in the setup, assuming non-minimal couplings.

Ashoorioon & Rezazadeh (2019)

- Whatever reason behind the smallness of quartic couplings, we assume they are small for phenomenological reasons.

Two-Field Cascading DE

- The system of $N+1$ fields will reduce to two-fields then,

$$H^2 = \frac{1}{3M_P^2}\left(\rho_{\rm m} + \rho_{\rm r} + \rho_\phi + \rho_\chi\right),$$

- In our work, we assume that all three families of neutrinos are massless.

- The first Friedmann equation takes the form

$$\tilde{H}^2 = \frac{4\left(\tilde{\rho}_{\rm mi} e^{-3N} + \tilde{\rho}_{\rm ri} e^{-4N}\right) + \tilde{\lambda}_\phi \tilde{\phi}^4 + \tilde{\lambda}_\chi \tilde{\chi}^4}{2\left(6 - \tilde{\phi}'^2 - \tilde{\chi}'^2\right)},$$

$$\tilde{H} \equiv \frac{H}{H_0}, \qquad \tilde{\phi} \equiv \frac{\phi}{M_P}, \qquad \tilde{\chi} \equiv \frac{\chi}{M_P},$$

$$\tilde{\lambda}_\phi \equiv \frac{M_P^2}{H_0^2}\lambda_\phi, \qquad \tilde{\lambda}_\chi \equiv \frac{M_P^2}{H_0^2}\lambda_\chi.$$

Two-Field Cascading DE

- The equations for ϕ and χ after some massage takes the form

$$\tilde{\phi}'' = -\frac{1}{6\tilde{H}^2}\left[e^{-4N}\tilde{\phi}'\left(3e^{4N}\tilde{H}^2\left(6-\tilde{\chi}'^2-\tilde{\phi}'^2\right) - 3\tilde{\rho}_{\rm mi}e^{N} - 4\tilde{\rho}_{\rm ri}\right) + 6\tilde{\lambda}_\phi\tilde{\phi}^3\right],$$

$$\tilde{\chi}'' = -\frac{1}{6\tilde{H}^2}\left[e^{-4N}\tilde{\chi}'\left(3e^{4N}\tilde{H}^2\left(6-\tilde{\chi}'^2-\tilde{\phi}'^2\right) - 3\tilde{\rho}_{\rm mi}e^{N} - 4\tilde{\rho}_{\rm ri}\right) + 6\tilde{\lambda}_\chi\tilde{\chi}^3\right].$$

- Assuming slow-roll in the initial time, we will have the following values for the initial quantities

$$\tilde{\phi}'_i \approx -\frac{4\tilde{\lambda}_\phi\tilde{\phi}_i^3}{4\left(\tilde{\rho}_{\rm mi}+\tilde{\rho}_{\rm ri}\right)+\tilde{\lambda}_\phi\tilde{\phi}_i^4+\tilde{\lambda}_\chi\tilde{\chi}_i^4},$$

$$\tilde{\chi}'_i \approx -\frac{4\tilde{\lambda}_\chi\tilde{\chi}_i^3}{4\left(\tilde{\rho}_{\rm mi}+\tilde{\rho}_{\rm ri}\right)+\tilde{\lambda}_\phi\tilde{\phi}_i^4+\tilde{\lambda}_\chi\tilde{\chi}_i^4}.$$

$$\tilde{H}_i^2 \approx \frac{4\left(\tilde{\rho}_{\rm mi}+\tilde{\rho}_{\rm ri}\right)+\tilde{\lambda}_\phi\tilde{\phi}_i^4+\tilde{\lambda}_\chi\tilde{\chi}_i^4}{2\left(6-\tilde{\phi}_i'^2-\tilde{\chi}_i'^2\right)}.$$

Two-Field Cascading DE

- To ensure flatness,

$$\Omega_{\mathrm{m}0} + \Omega_{\mathrm{r}0} + \Omega_{\phi 0} + \Omega_{\chi 0} = 1,$$

which relates

$$\tilde{\lambda}_\phi = \frac{12 - \tilde{\lambda}_\phi \tilde{\chi}_0^4 - 2\tilde{\phi}_0'^2 - 2\tilde{\chi}_0'^2 - 12\Omega_{\mathrm{m}0} - 12\Omega_{\mathrm{r}0}}{\tilde{\phi}_0^4}.$$

We used shooting method to fix $\tilde{\lambda}_\phi$ as a derived parameter.

Numerical Results

- We use the CosmoMC code to constrain our CDE model at the level of background.

- The parameters in our model is $\{\Omega_b h^2, \Omega_c h^2, \theta_{MC}, \tau, A_s, n_s, \tilde{\phi}_i, \tilde{\chi}_i, \tilde{\lambda}_\chi\}$
- θ_{MC} refers to the ratio of the comoving sound horizon at decoupling to the comoving angular diameter distance to the surface of last scattering
- We suppose flat priors on the free parameters on $\tilde{\chi}_i$ and $\log \tilde{\lambda}_\chi$ and $\log \tilde{\phi}_i$.

- We include the combination of CMB temperature and polarization, SNe Ia, BAO, and Riess et al. (2019) dataset in our work, and so multiplying the separate likelihoods for these datasets, the total likelihood will be $\mathscr{L} \propto e^{-\chi^2_{\rm tot}/2}$ where $\chi^2_{\rm tot} = \chi^2_{\rm CMB} + \chi^2_{\rm SN} + \chi^2_{\rm BAO} + \chi^2_{\rm Riess2019}$

- We terminate the MCMC analysis when $|R-1| < 0.1$, where R is the Gelman-Rubin parameter.

Numerical Results

- We incorporate the Planck 2018 CMB data for the temperature and polarization at small (TT,TE,EE) and large (lowl+lowE) angular scales.

- We additionally take into account the CMB lensing potential power spectrum measured in the multipole range $40 \leq \ell \leq 400$.

- The locations of the peaks are sensitive to the physical processes from the time of decoupling to today.

- We take into account 1048 Pantheon SNe Ia $0.01 < z < 2.3$

- We incorporate BAO data points in our numerical analysis from BOSS DR12, SDSS Main Galaxy Sample, and 6dFGS.

- we include the Riess et al. (2019) measurement, $H_0 = 74.03 \pm 1.42\,\mathrm{km\,s^{-1}\,Mpc^{-1}}$ for the Hubble constant, which is derived from the Hubble Space Telescope (HST) observations of 70 long-period Cepheids in the Large Magellanic Cloud

Numerical Results

TABLE I. The best fit values and 68% CL constraints for the parameters of the investigated models.

Parameter	ΛCDM		Single-field DE		Rock 'n' Roll		Two-field CDE	
	best-fit	68% limits	best-fit	68% limits	best-fit	68% limits	best-fit	68% limits
$\Omega_b h^2$	0.0226089	0.02251 ± 0.00013	0.0225312	0.02251 ± 0.00013	0.0228385	0.02280 ± 0.00015	0.0227861	0.02282 ± 0.00016
$\Omega_c h^2$	0.11827	0.11849 ± 0.00090	0.118691	0.11851 ± 0.00087	0.121385	$0.1222^{+0.0011}_{-0.0014}$	0.122667	$0.1222^{+0.0012}_{-0.0015}$
$100\theta_{\rm MC}$	1.04116	1.04116 ± 0.00029	1.04108	1.04113 ± 0.00029	1.03951	$1.03942^{+0.00060}_{-0.00042}$	1.0396	$1.03939^{+0.00063}_{-0.00043}$
τ	0.0596178	0.0568 ± 0.0071	0.0572416	$0.0566^{+0.0064}_{-0.0072}$	0.054335	0.0529 ± 0.0071	0.0492794	0.0532 ± 0.0072
$\ln(10^{10} A_s)$	3.04763	3.046 ± 0.014	3.04411	$3.046^{+0.013}_{-0.014}$	3.04998	3.046 ± 0.014	3.04385	3.046 ± 0.014
n_s	0.968599	0.9690 ± 0.0037	0.969799	0.9688 ± 0.0036	0.968158	0.9688 ± 0.0037	0.967781	0.9691 ± 0.0037
$\log(\tilde{\phi}_i)$	–	–	1.81705	$2.56^{+1.3}_{-0.57}$	–	–	3.13425	> 1.76
$\tilde{\chi}_i$	–	–	–	–	0.480162	< 0.523	0.484908	$0.502^{+0.033}_{-0.096}$
$\log(\tilde{\lambda}_\chi)$	–	–	–	–	15.3182	–	15.4771	–
H_0	68.7567	68.60 ± 0.41	68.5669	68.60 ± 0.41	70.9546	$70.94^{+0.58}_{-0.84}$	70.5298	$70.95^{+0.61}_{-0.85}$
$\Omega_{\rm m}$	0.297999	0.7003 ± 0.0052	0.300383	0.2997 ± 0.0051	0.286467	0.2883 ± 0.0057	0.292401	0.2883 ± 0.0058
$\Omega_{\rm DE}$	0.702001	0.2997 ± 0.0052	0.699617	0.7003 ± 0.0051	0.713533	0.7117 ± 0.0057	0.707599	0.7117 ± 0.0058
σ_8	0.820063	0.8208 ± 0.0060	0.821043	0.8208 ± 0.0058	0.839236	$0.8417^{+0.0072}_{-0.0087}$	0.841436	$0.8415^{+0.0075}_{-0.0087}$
S_8	0.817324	0.820 ± 0.010	0.821567	0.8204 ± 0.0098	0.820089	0.825 ± 0.010	0.830711	0.825 ± 0.010
$\log(\tilde{\lambda}_\phi)$	–	–	−6.34384	$-9.3^{+4.1}_{-4.8}$	–	–	−11.6081	-8.5 ± 3.7

Parameter	ΛCDM		Single-field DE		Rock 'n' Roll		Two-field CDE	
	best-fit	68% limits	best-fit	68% limits	best-fit	68% limits	best-fit	68% limits
$\chi^2_{\rm CMB}$	2777.72	2788.9 ± 5.9	2777.19	2788.9 ± 6.0	2777.13	2790.7 ± 6.1	2777.35	2790.7 ± 6.0
$\chi^2_{\rm SN}$	1034.74	1034.792 ± 0.083	1034.74	1034.80 ± 0.12	1035.07	1035.05 ± 0.29	1034.82	1035.05 ± 0.32
$\chi^2_{\rm BAO}$	5.77561	5.89 ± 0.81	5.44215	5.86 ± 0.82	8.63314	8.4 ± 2.2	6.61057	8.4 ± 2.2
$\chi^2_{\rm Riess2019}$	13.7907	14.7 ± 2.2	14.8014	14.7 ± 2.2	4.69061	5.0 ± 2.1	6.07593	5.0 ± 2.2
$\chi^2_{\rm total}$	3832.03	–	3832.17	–	3825.52	–	3824.86	–
$\Delta\chi^2$	0.0	–	0.14	–	−6.51	–	−7.17	–

Numerical Results

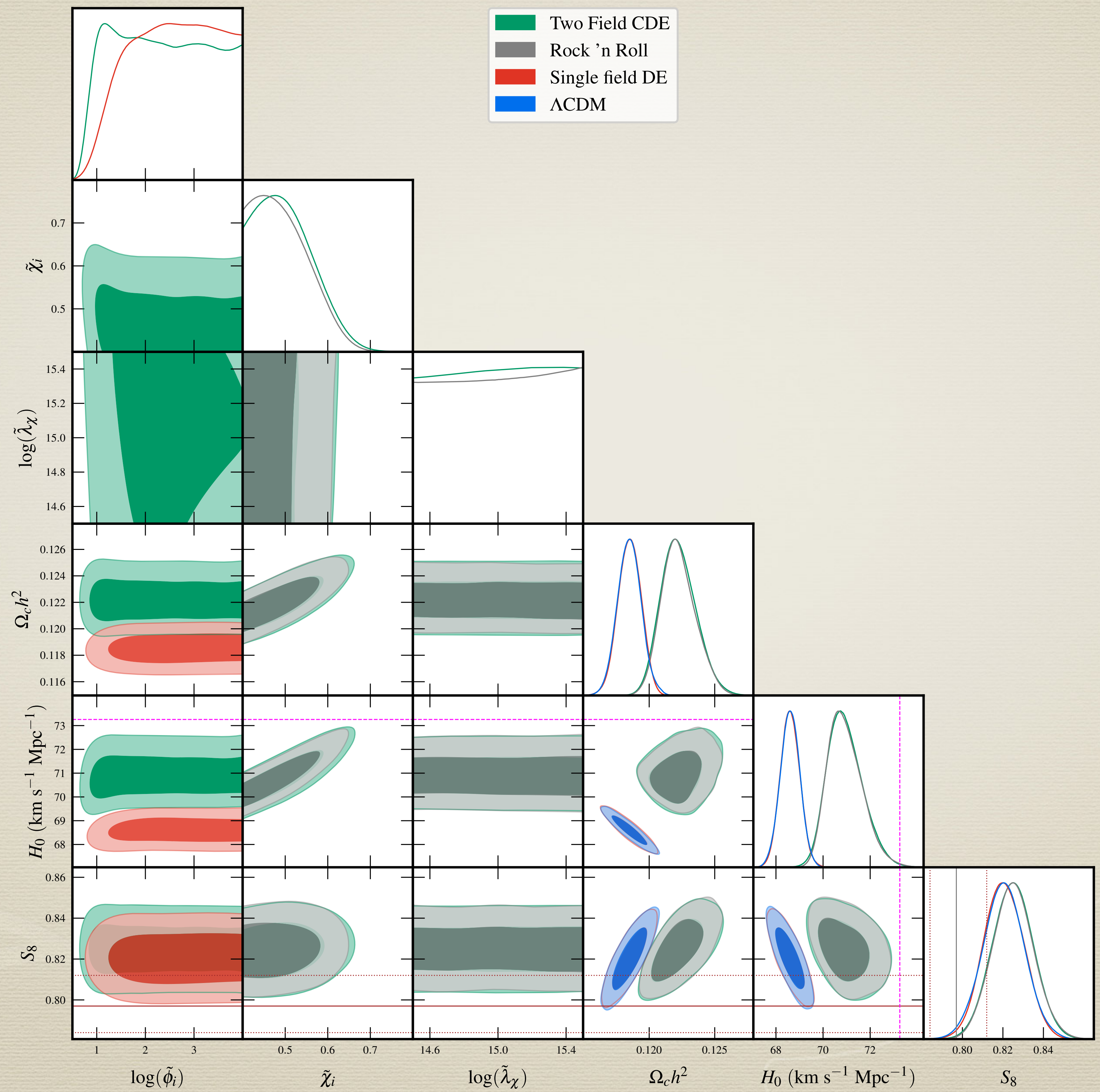

Numerical Results

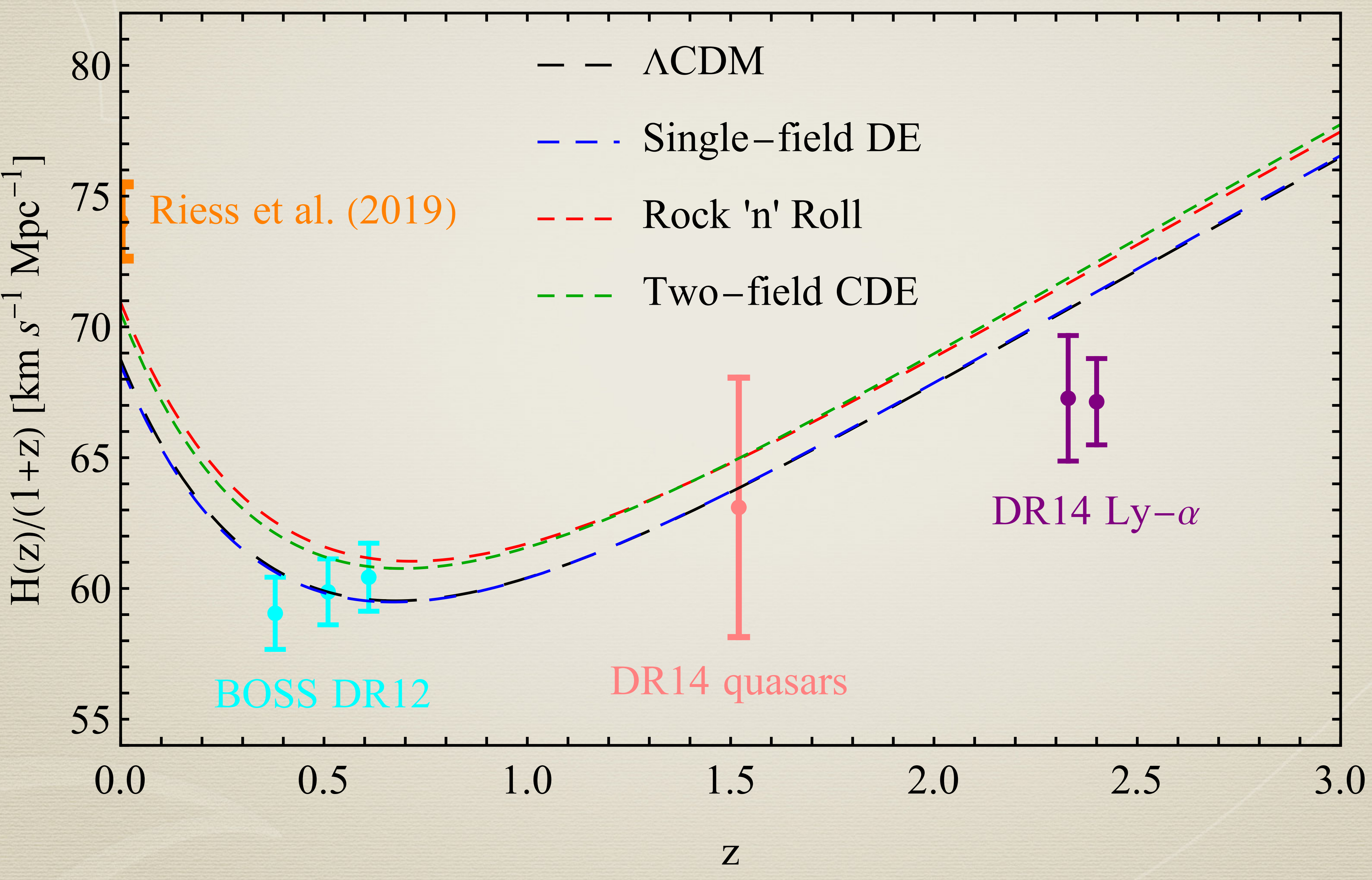

Numerical Results

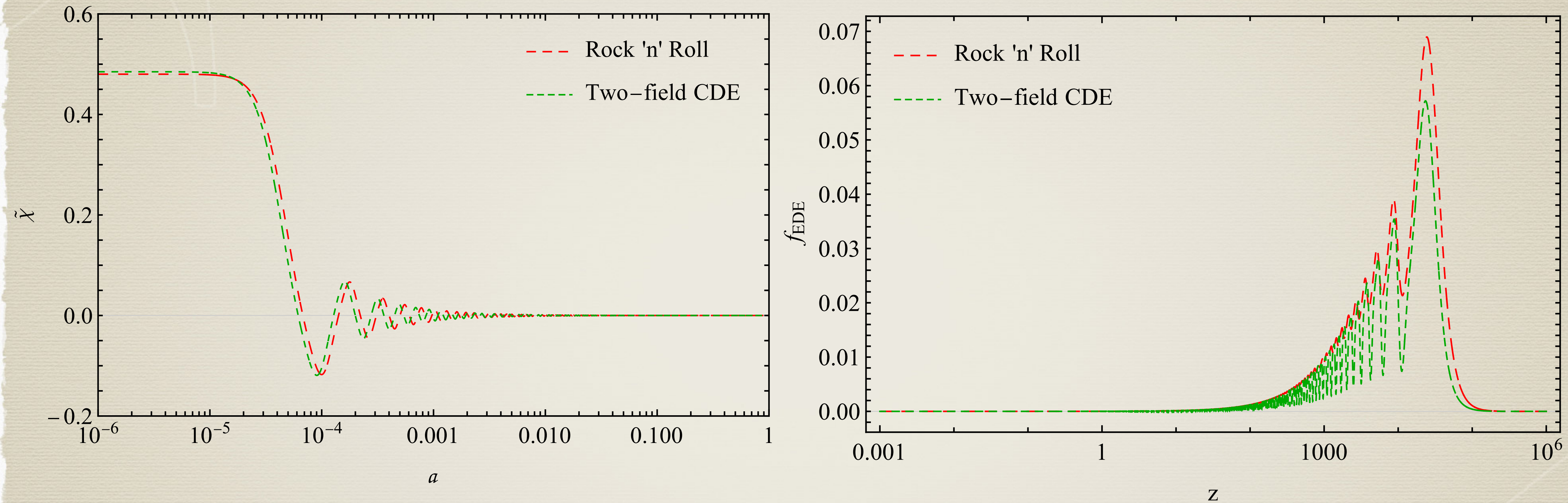

For the rock `n' roll model, the peak appears at the critical redshift $z_c = 2.44 \times 10^4$ with the maximum value $f_{\mathrm{EDE}} = 0.069$. The peak of the two-field CDE model appears at $z_c = 2.34 \times 10^4$ with the maximum amplitude $f_{\mathrm{EDE}} = 0.057$.

Numerical Results

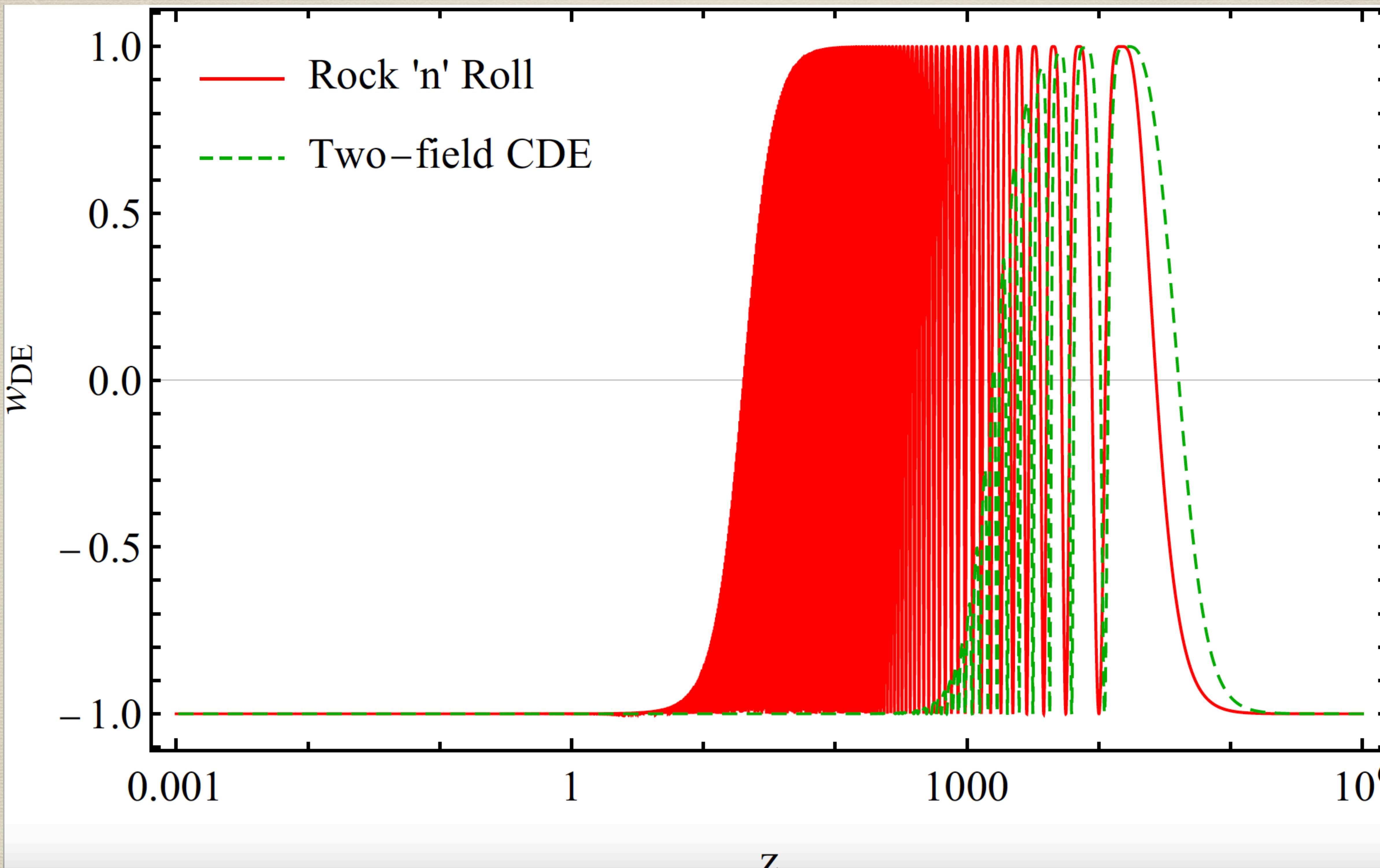

Conclusions and Future Research

- Cascading Dark Energy provides a mechanism to better understand the origin of H_0 tension in the context of fundamental physics.
- Late-time accelerated expansion results from the cooperation of many fields, some of which are not in tune with the rest of the band and *cascades.*
- If the cascade process happens once, it can be shown that the model effectively reduces to a two-field cascading dark energy model.
- If the cascade process happens once, it can be shown that the model effectively reduces to a two-field cascading dark energy model.
- We used MCMC with a host of CMB, Pantheon, BAO, SNe Ia, Reiss 2019 data, to examine our model against the data.

Conclusions and Future Research

- We noticed that our model with both early and late dark energy evolution outperforms the rock and roll model.

- Specifically for BAO data, our model inherits the preference the evolving DE has over the cosmological constant.

- Our cascading model not only beats the ΛCDM and single field DE model, but also the rock `n’ roll model

- Our prediction for z_c, where the fraction of EDE becomes maximum is some different from previous estimates of this parameters. In our case this happens around $z_c \approx 2.44 \times 10^4$

Thanks for your attention!